# NATIONAL ADVISORY COMMITTEE FOR AERONAUTICS

# WARTIME REPORT

### ORIGINALLY ISSUED

July 1944 as
Memorandum Report

WIND-TUNNEL INVESTIGATION OF THE EFFECT OF JET-MOTOR

OPERATION ON STABILITY

By Wallace F. Davis and Sherwood H. Brown

Ames Aeronautical Laboratory
Moffett Field, California

## NACA

### WASHINGTON

NATIONAL ADVISORY COMMITTEE FOR AERONAUTICS

# WIND-TUNNEL INVESTIGATION OF THE EFFECT OF JET-MOTOR

## OPERATION ON STABILITY

By Wallace F. Davis and Sherwood H. Brown

## SUMMARY

The effects of jet-motor operation on the stability and control characteristics of two fighter-type airplanes as determined by wind-tunnel tests of 1/5-scale models are presented. It is shown that the action of the jets is to cause a small loss in stick-fixed stability which is predictable from known theories.

## INTRODUCTION

A jet-propulsion engine draws air into a compressor and delivers it to a chamber where the addition and combustion of fuel results in a high-temperature gaseous mixture under high pressure. This mixture is then partially expanded through a gas turbine and is finally ejected as a high-velocity high-temperature jet. In general, the diffusion of such a jet is the result of the absorption of its energy by the surrounding fluid through turbulent mixing. The diameter of the jet increases slowly at a maximum diffusion angle of about $7^\circ$ (references 1 and 2) and the increase in cross-sectional area is accompanied by a decrease in velocity. If the momentum of the spreading jet is to remain constant, the decrease in velocity must be accompanied by an increase in mass flow. This means, of course, that part of the fluid in the surrounding stream is drawn into the jet and the streamlines of the stream are deflected toward the axis of the high-velocity jet. Theoretical treatments of this flow problem are given in reference 3.

Prior to the development of these theoretical studies, tests of models of two fighter-type airplanes, one with a single jet motor discharging its hot gases from the tail and the other a twin-engine airplane with jets exhausting near the wing roots, were made in the Ames 7- by 10-foot wind tunnels to determine the effects of jet operation on stability and control. This report presents the results of these tests with

a cold jet and compares them with the change in stability calculated from theory.

## JET-PROPULSION SIMULATION

If actual jet-propulsion engine-operating conditions were to be used in wind-tunnel testing, a jet of the same outlet velocity and temperature as generated by the full-scale engine would be necessary. The difficulties met in producing these conditions in a wind-tunnel model have made actual simulation impractical at the present time, so the following approximate method has been developed.

If it is assumed that jet operation does not affect the external drag of the engine housing and that the static pressure at the jet outlet is equal to atmospheric pressure, the thrust of a jet-propulsion unit will be equal to the rate of change in the momentum of the fluid emerging from the jet or

$$T = M_A (V_J - V) + M_F V_J$$

where

$T$      thrust force, pounds

$M_A$      mass flow of air, slugs per second

$V_J$      velocity of fluid at jet outlet, feet per second

$V$      velocity of flight, feet per second

$M_F$      mass flow of fuel, slugs per second

Then, defining the jet thrust coefficient $T_{C_J}'$ as the thrust divided by the product of the dynamic pressure of the free stream $q$ (lb/sq ft) and the wing area $S$ (sq ft),

$$T_{C_J}' = \frac{T}{qS} = \left( \frac{M_A + M_F}{M_A + M_F} \right) \left( \frac{M_A (V_J - V) + M_F V_J}{\rho \frac{V^2 S}{2}} \right)$$

and since

$$M_A + M_F = \rho_J V_J A_J$$

where

$\rho_J$     density of fluid at jet outlet, slugs per cubic foot

$A_J$     area of jet outlet, square feet

$$T_{c_J}' = 2 \left( \frac{M_A}{M_A + M_F} \right) \frac{\rho_J V_J A_J (V_J - V)}{\rho V^2 S} + 2 \left( \frac{M_F}{M_A + M_F} \right) \frac{\rho_J V_J^2 A_J}{\rho V^2 S}$$

$$= 2 \frac{\rho_J V_J A_J}{\rho V^2 S} \left[ V_J \left( \frac{M_A + M_F}{M_A + M_F} \right) - V \left( \frac{M_A}{M_A + M_F} \right) \right]$$

$$= 2 \frac{\rho_J A_J}{\rho S} \left[ \left( \frac{V_J}{V} \right)^2 - \frac{V_J}{V} \left( \frac{M_A}{M_A + M_F} \right) \right]$$

With the jet-propulsion engines used at the present time $M_F$ will not be more than 2 percent of $M_A$ even under extreme conditions. Therefore, if $M_F$ is neglected,

$$T_{c_J}' = 2 \left( \frac{\rho_J}{\rho} \right) \left( \frac{A_J}{S} \right) \left( \frac{V_J}{V} \right) \left[ \frac{V_J}{V} - 1 \right]$$

and the thrust will be simulated if the product of the ratios of the above equation is the desired constant. If a cold jet is used in wind-tunnel testing, the density ratio will not be the same as found under actual conditions; however, a given $T_{c_J}'$ can be obtained by adjusting the value of $A_J/S$. This adjustment was made in the case of the models by reducing the jet-outlet area with a streamlined plug.

The principal sources of error in using this method of jet simulation are the incorrect jet temperature and viscosity and the change in the manner of jet diffusion by the stream-lined plug. Both of these errors will affect the inflow about the jet, and thus possibly the stability and control characteristics of a wind-tunnel model. However, it is believed that these errors will be small and of secondary importance.

4

## APPARATUS AND METHOD

The arrangement of the 1/5-scale models of the fighter airplanes in the 7- by 10-foot wind tunnel is shown in figures 1 and 2 and the model dimensions are given in figures 3 and 4. The jet was simulated by compressed air supplied to the model by the piping arrangement shown in figures 1 and 2. This air passed through a mercury seal that removed any restraint from the balance system and entered the floating frame along the center line of rotation in yaw perpendicular to the drag and cross-force-wind axes and along the axis of the links of the front-lift scales. The model pitched about a fixed vertical pipe, and the rotation of the jet outlet about the pivot was taken by flexible tubing. In order to reduce interference and tare forces, the length of the pipe that projected into the wind-tunnel air stream was surrounded by a fairing that was free of the wind-tunnel balance system. The jet-outlet velocity was calculated from measurements obtained from a thermocouple and calibrated orifices in the pipe leading to the jet outlet.

The forces due to jet operation were measured through the available jet-velocity range (0 to 1000 ft/sec) in a tunnel-off calibration. Since only the effects of the change in flow about the model were desired, the pitching moment and the force components resulting from the thrust of the jet have been subtracted from the test results. All the data have been corrected for wind-tunnel-wall effects and tares.

The method of conducting the tests consisted of setting the outlet velocity of the jet at the highest attainable value and varying the outlet-velocity ratio $V_J/V$ by changing the dynamic pressure in the wind tunnel. This procedure caused a change in Reynolds number (from 700,000 to 1,700,000, based upon the mean aerodynamic chord of the models) that affected the aerodynamic characteristics of the models to some extent, especially when the flaps were deflected. In order to eliminate this variable, jet-off data were obtained at the same dynamic pressures as were the jet-on data. Comparison of the results showed an increment in pitching moment and control hinge moment due to jet operation. In order to illustrate the effect of outlet-velocity ratio, it has been assumed that Reynolds number has a negligible effect on these increments, and they have been added to the basic moment and hinge-moment curves obtained at the higher Reynolds number.

The nature of the flow in the region of a high-velocity jet was investigated by visual and qualitative observations. The apparatus for the former method consisted of a 5-inch by 5-inch plexiglass flow channel, a two-dimensional jet, and a

smoke generator. The jet was supplied by compressed air from a source of variable pressure and issued from a 1/16-inch slot in a plenum chamber that extended across the flow channel. Smoke was produced by blowing an oil mixture through a heated coil and was introduced into the low-velocity air stream (6 to 12 ft/sec) above the jet outlet. High-speed photographs were taken of the smoke streamers through an outlet-velocity ratio range of 0 to 8.

The magnitude and the direction of the change in flow about the jet outlet of the single-engine airplane model were measured with a directional pitot-tube. The accuracy of this instrument in measuring angles of pitch and yaw is within about ±0.25°, and the dynamic pressure measurements are within about ±1 percent.

The change in pressure distribution on the horizontal tail surface of the single-engine fighter model was measured by static pressure orifices at 25 percent and 50 percent of the elevator semispan on an airfoil located 6 inches (model scale) above the center line of the jet outlet.

## RESULTS AND DISCUSSION

### Flow Pattern

Since the high-velocity jets of both airplanes could influence the flow in the vicinity of the tail and thereby change the stability, tests were made in a small flow channel to study the flow around the jet with smoke streamers. Figure 5 shows photographs of these smoke streamers. These studies indicate that the streamlines curve toward the jet as the outlet-velocity ratio is increased and that the greatest change in stream direction is near the jet outlet. Measurements, with a directional pitot tube, of the magnitude of the flow-angle changes about the jet of the single-engine airplane model are not of sufficient accuracy to determine absolute values, since the variation is of the same magnitude as the accuracy of the instrument. However, the data of figure 6 do show that the change in stream direction in the region of the horizontal surface is small (less than 1°). No measurable change in the velocity of the stream at the tail was noticed.

### Change in Tail Load

The flow inclination caused by the jet produced an increase in the download on the horizontal tail of the single-engine airplane model because of an increase in

downwash angle and a change in the effective camber of the airfoil section. Measurements of the pressure-coefficient $(P = \Delta P/q)$ distribution show that the jet causes a decrease in the pressure on the lower surface that increases with jet thrust coefficient $(T_{cJ}')$ and decreases with distance from the center line of the jet. (See fig. 7.) The change in pressure coefficient is small, being equal to about 0.15 at 25 percent of the semispan of the horizontal tail for an outlet-velocity ratio of 12.

A decrease in pressure on the lower surface of the horizontal tail causes a more positive pitching-moment coefficient. Measurements of the pitching moment with the same horizontal tail as was used for the pressure-distribution tests showed a positive shift of the pitching-moment-coefficient curve of about 0.03 at an outlet-velocity ratio of 12. Since the pitching moment of the model without a tail was not affected by jet operation, this change in $C_m$ agreed with that predicted by the pressure measurements.

## Change in Longitudinal Stability

For the single-engine model, military-rated-power operation of the jet-propulsion engine of the airplane is characterized by the variation of thrust coefficient $T_{cJ}'$ and outlet-velocity ratio $V_J/V$ with speed that is shown in figure 8. The variations of pitching-moment and elevator hinge-moment coefficients resulting from operation of the jet are shown in figure 9, 10, and 11. From these data, the effect of jet operation upon an 8000-pound single-engine airplane flying at sea level has been computed and is summarized in the following table:

| Condition | Measured change in stick-fixed neutral-point location | Estimated change in neutral-point location (from ref. 3). |
|---|---|---|
| Flaps retracted | 2 percent M.A.C. | 2 percent M.A.C. |
| Flaps 55° | 1 percent M.A.C. | ------------------ |

For the twin-engine airplane, the variation of outlet-velocity ratio, thrust coefficient, and lift coefficient with airspeed are given in figure 12. Figures 13, 14, and 15 show the effects of jet operation on the stability and control and

elevator hinge moments. The measured and estimated changes in stick-fixed stability for the twin-engine airplane are given in the following table:

| Condition | Measured change in stick-fixed neutral point location | Estimated change in neutral point location (from reference 3). |
|---|---|---|
| Flaps retracted | 3 percent M.A.C. | 4.2 percent M.A.C. |
| Flaps deflected | 4 percent M.A.C. | ------------------- |

From these data it is concluded that the effects of jet operation on the stick-fixed stability are small and may be predicted with reasonable accuracy from known theories.

The effects of jet operation on the elevator hinge moments of the single-engine airplane result in an increase in stick-free stability because of the increase in $C_{h_\alpha}$. Calculated stick-free neutral-point shifts of 30 percent for this condition are not of significance, however, since the force variation with speed is very slightly increased. For the twin-engine airplane the effect of jet operation on the hinge-moment characteristics is negligible, insofar as changes in stick-free stability are concerned.

## Directional Stability

Tests of the directional stability with jets operating show negligible changes in stability and trim.

## CONCLUDING REMARKS

It is concluded that the effects of jet operation on the stability characteristics of airplanes similar to those for which model tests were made will be small provided the jet does not impinge on the tail. The stability changes can be predicted with reasonable accuracy from known theories. It is possible that for certain locations of the tail plane relative to the jet, stability changes appreciably greater than those found for the models of this report may be

8

experienced.  Study of the theoretical treatises will show
regions of large flow angles which should be avoided in
fixing the position of the tail.


Ames Aeronautical Laboratory,
    National Advisory Committee for Aeronautics,
        Moffett Field, Calif., Nov. 8, 1945.


## REFERENCES

1.  Corrsin, Stanley:  Investigation of Flow in an Axially
        Symmetrical Heated Jet of Air.  NACA ACR No. 3L23, 1943.

2.  Abramovich, G. N.:  The Theory of a Free Jet of a
        Compressible Gas.  NACA TN No. 1058, 1944.

3.  Ribner, Herbert S.:  Field of Flow About a Jet and Effect
        of Jets on Stability of Jet-Propelled Aircraft.
        MR L5E01, 1945.

FLEXIBLE TUBING

STREAMLINED PLUG
FOR JET SIMULATION

STATIC PRESSURE ORIFICES

THERMOCOUPLE

STREAMLINED FAIRING

FLOATING FRAME

DRAG SCALE LINK

SUPERCHARGER

WALL OF TEST CHAMBER

FRONT LIFT
SCALE LINKS

REAR LIFT
SCALE LINK
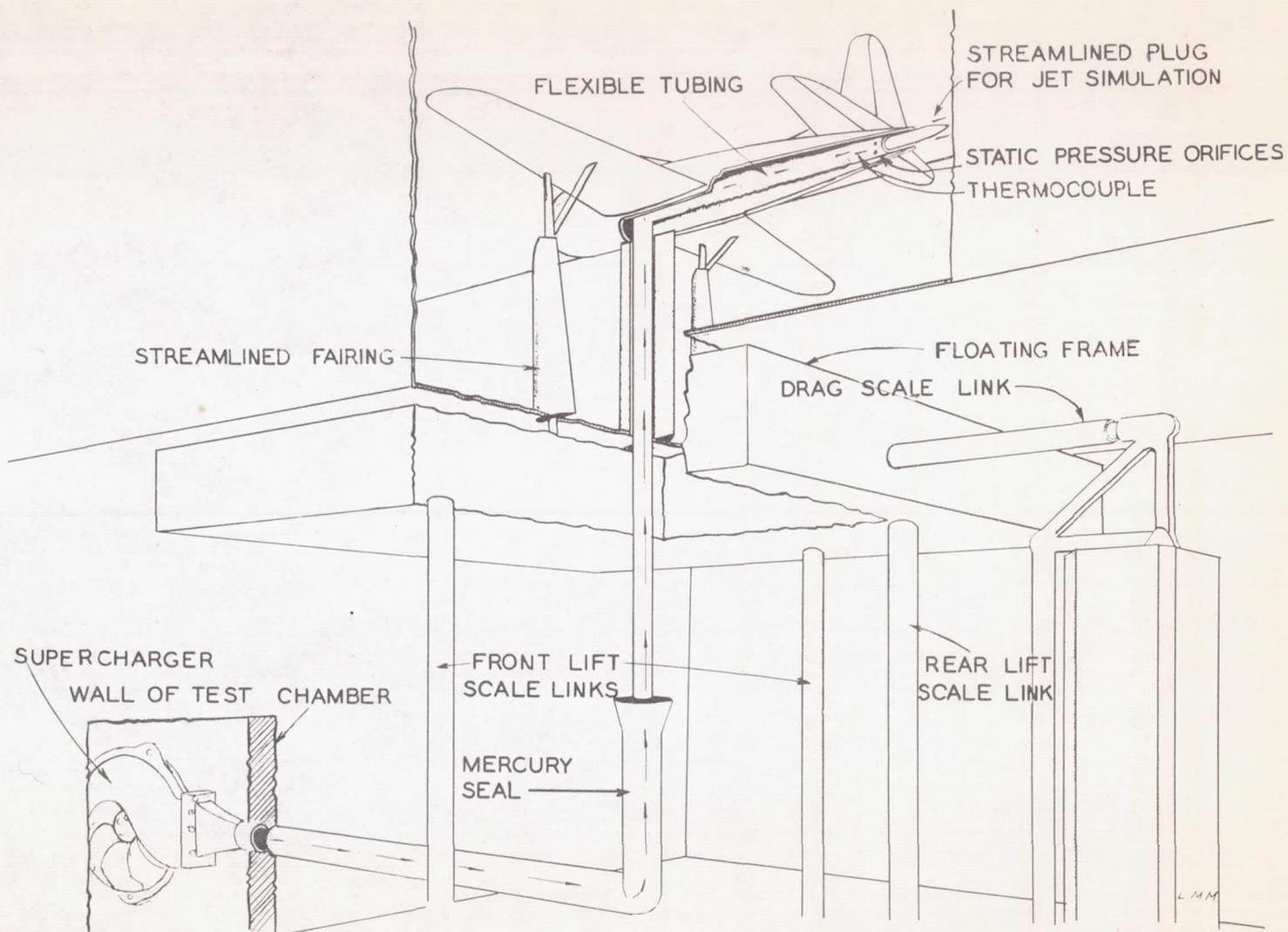
MERCURY
SEAL

FIGURE I.— METHOD OF SUPPLYING THE JET OF THE SINGLE-ENGINE AIRPLANE MODEL

WITH COMPRESSED AIR.

NACA
A-8968
11-6-45
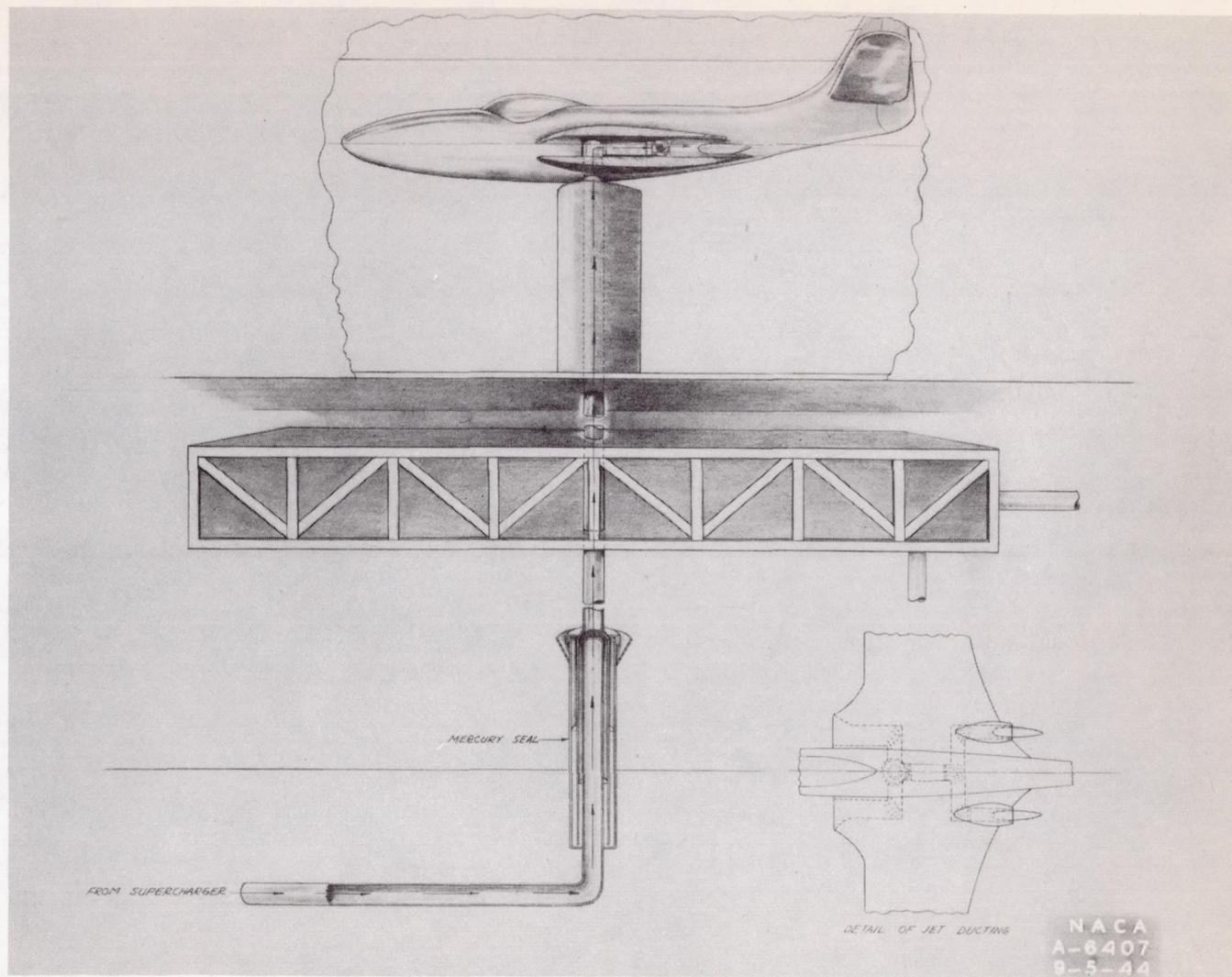
Figure 2.- Sketch of air ducts and mercury seal for 1/5-scale model of the two-engine airplane.

FIGURE 3.— DIMENSIONS OF THE SINGLE-ENGINE AIRPLANE MODEL.

NATIONAL ADVISORY
COMMITTEE FOR AERONAUTICS

ELEVATORS-SEALED GAP,
50% INTERNAL BALANCE

¢ ELEV. HINGE

42.

7.8

11.7

49.4

.69

22.2

22.4

11.2

19.8

17.45

WING
INCIDENCE +1°

96

7°30' DIHEDRAL
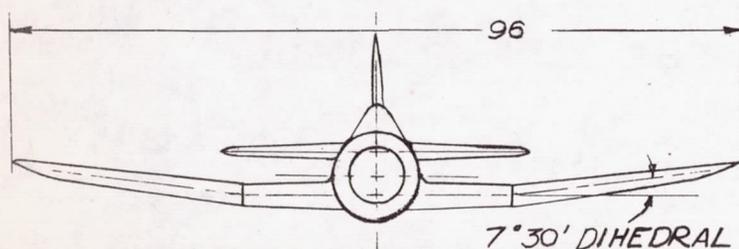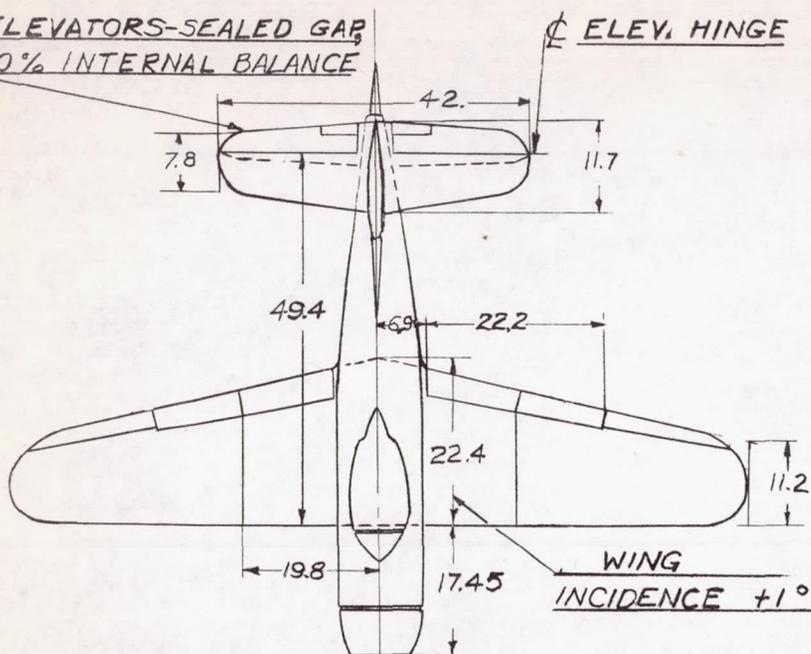
ALL DIMENSIONS ARE IN INCHES.

¢ THRUST

JET DIA. 2.50

JET PLUG DIA. 2.09

2.7

2.9

72.05

**MODEL DIMENSIONS**

WING AREA = 11.00 SQ. FT.
MAC = 19.31 IN.
HORIZONTAL TAIL AREA = 2.754 SQ. FT.
HORIZONTAL TAIL ASPECT RATIO = 4.45
ELEVATOR CHORD = .35 c (.273 FT. AV.)
ELEVATOR AREA AFT OF $H_l$ = .834 SQ. FT.
ELEVATOR BALANCE CHORD = .50 $c_e$
NORMAL C.G. 20% M.A.C. AFT OF M.A.C. L.E.
NORMAL C.G. 0.86% M.A.C. ABOVE THRUST LINE
NORMAL C.G. TO ELEVATOR HINGE LINE = 45.54 IN.
DOUBLE SLOTTED FLAPS   25% WING CHORD

MODEL DIMENSIONS

WING AREA = 11.05 SQ. FT.
M.A.C. = 16.92 IN.
HORIZONTAL TAIL AREA = 2.27 SQ. FT.
HORIZONTAL TAIL ASPECT RATIO = 3.84
ELEVATOR CHORD .388 c (.292 FT. AV.)
ELEVATOR AREA AFT OF $H$ .79 SQ. FT.
ELEVATOR BALANCE CHORD .35 $c_e$
NORMAL C.G. 18.6% M.A.C. AFT. OF M.A.C. L.E.
NORMAL C.G. 1.18% M.A.C. ABOVE THRUST LINE
NORMAL C.G. TO ELEVATOR HINGE LINE 3.60 FT.
SPLIT FLAPS

35.4"
4.7"
1.2"
8.19
12.0"
22.2"
JET DIA = 2.8"
JET PLUG DIA = 2.45"
1½°
.62"

NATIONAL ADVISORY
COMMITTEE FOR AERONAUTICS

100.8"
89.3"
31.6"
7.1"
THRUST LINE
10° DIHEDRAL
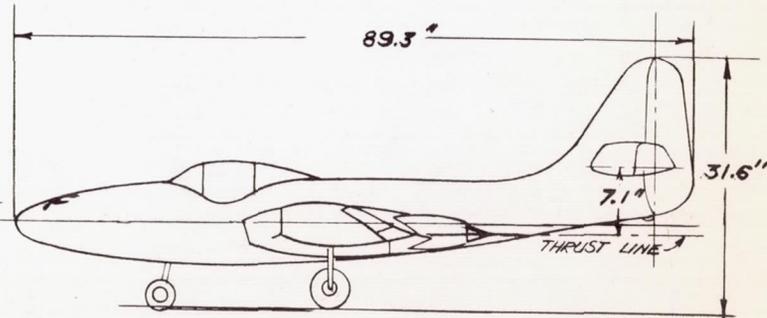
FIGURE 4 - THREE-VIEW DRAWING OF TWO-ENGINE AIRPLANE MODEL.
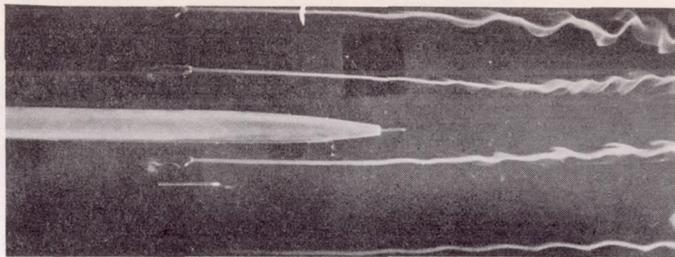
$V_J/V = 0$      $V = 6.6$ fps
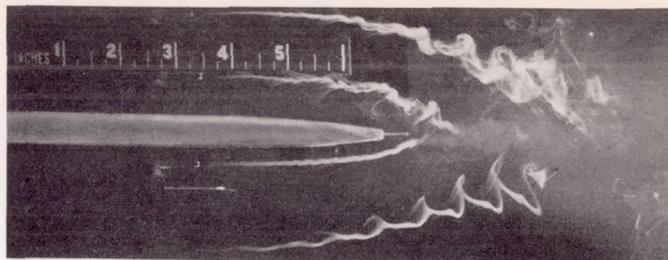
$V_J/V = 6.3$      $V = 8.6$ fps
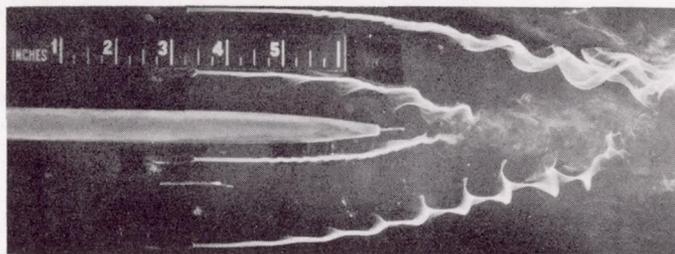
$V_J/V = 2.6$      $V = 6.9$ fps
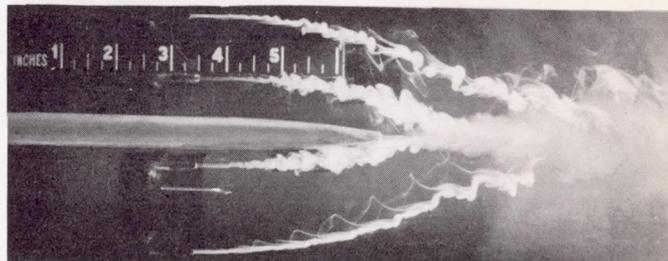
$V_J/V = 6.7$      $V = 10.7$ fps
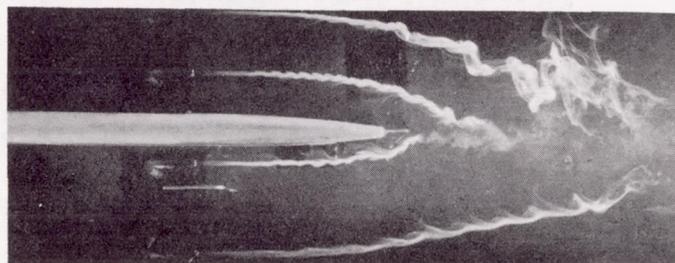
$V_J/V = 4.4$      $V = 8.1$ fps
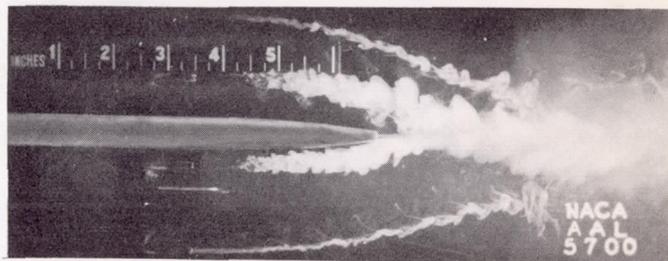
$V_J/V = 7.8$      $V = 11.7$ fps

Figure 5.- Photographs of smoke streamers showing the effect of a two-dimensional jet upon the surrounding field of flow through an outlet-velocity ratio range from 0 to 8.
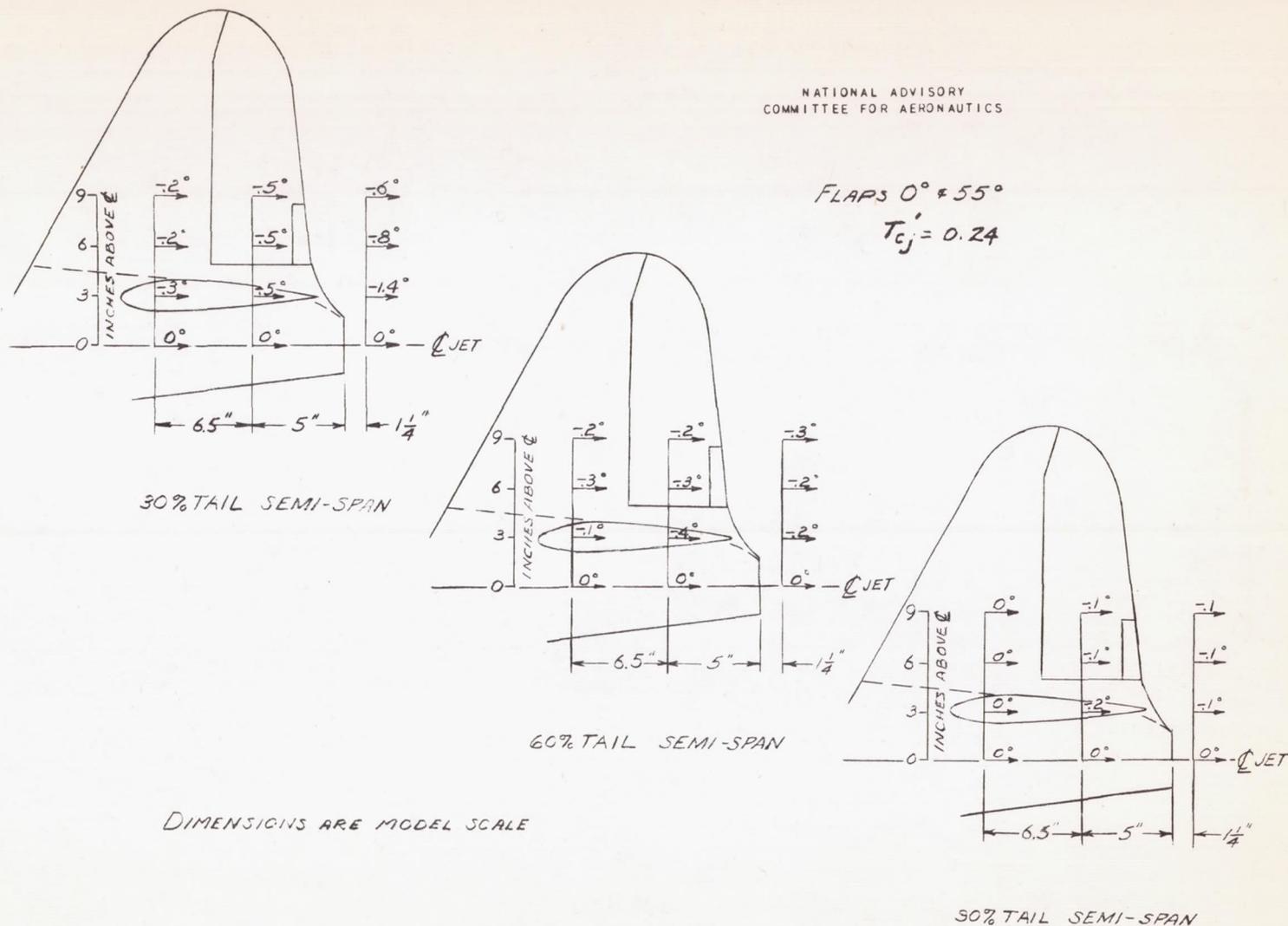
FIGURE 6.— THE CHANGE OF STREAM DIRECTION RESULTING FROM OPERATION OF THE JET-PROPULSION UNIT OF THE SINGLE-ENGINE AIRPLANE MODEL.

25% SEMI-SPAN

50% SEMI-SPAN
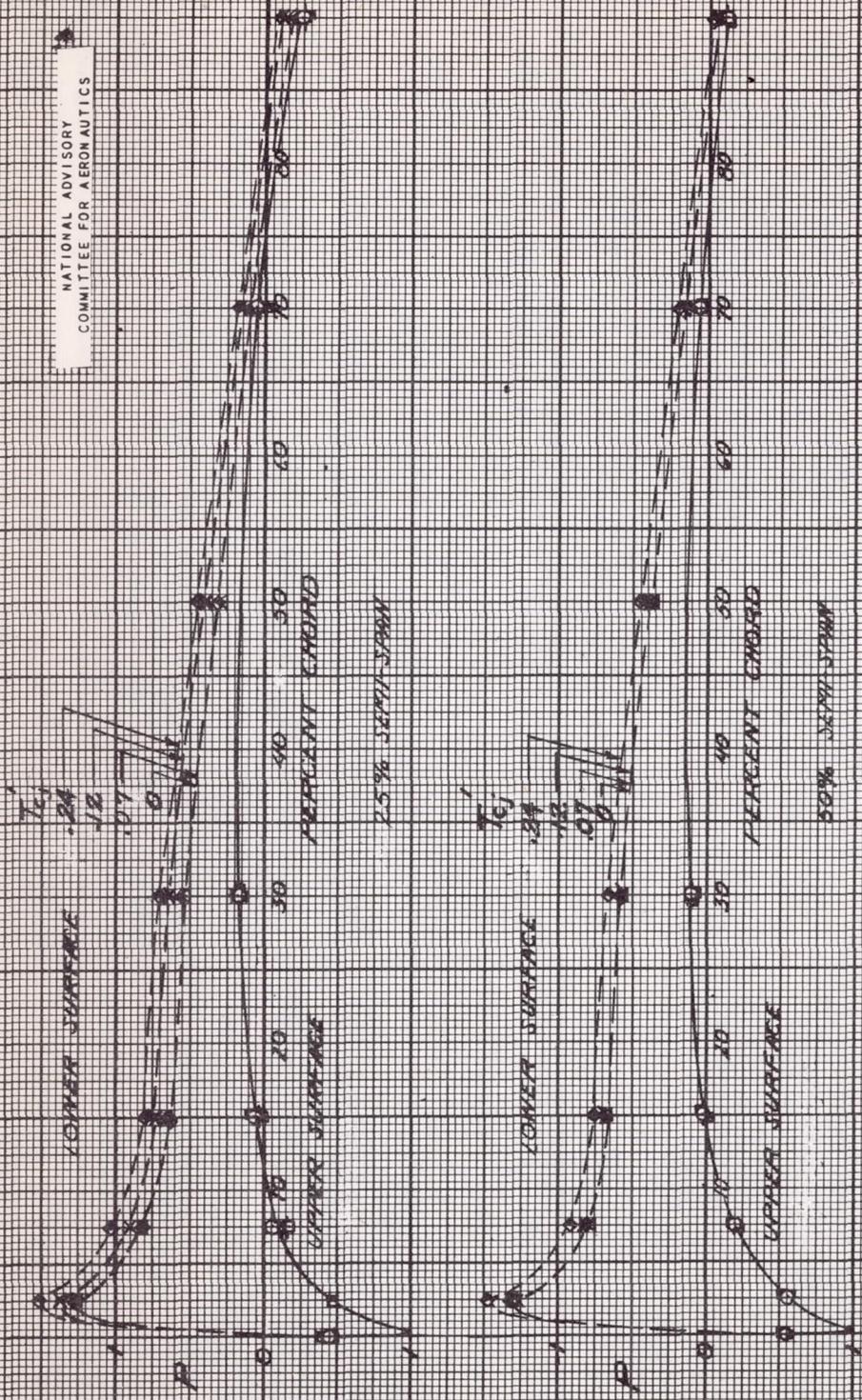
FIGURE 7.— THE EFFECT OF JET-THRUST COEFFICIENT ON THE PRESSURE
DISTRIBUTION OVER THE HORIZONTAL TAIL OF THE SINGLE-ENGINE
AIRPLANE MODEL.

FLAPS 55°,     αₜ=4°,     δₜ=1.49     TAIL INCIDENCE 1°.
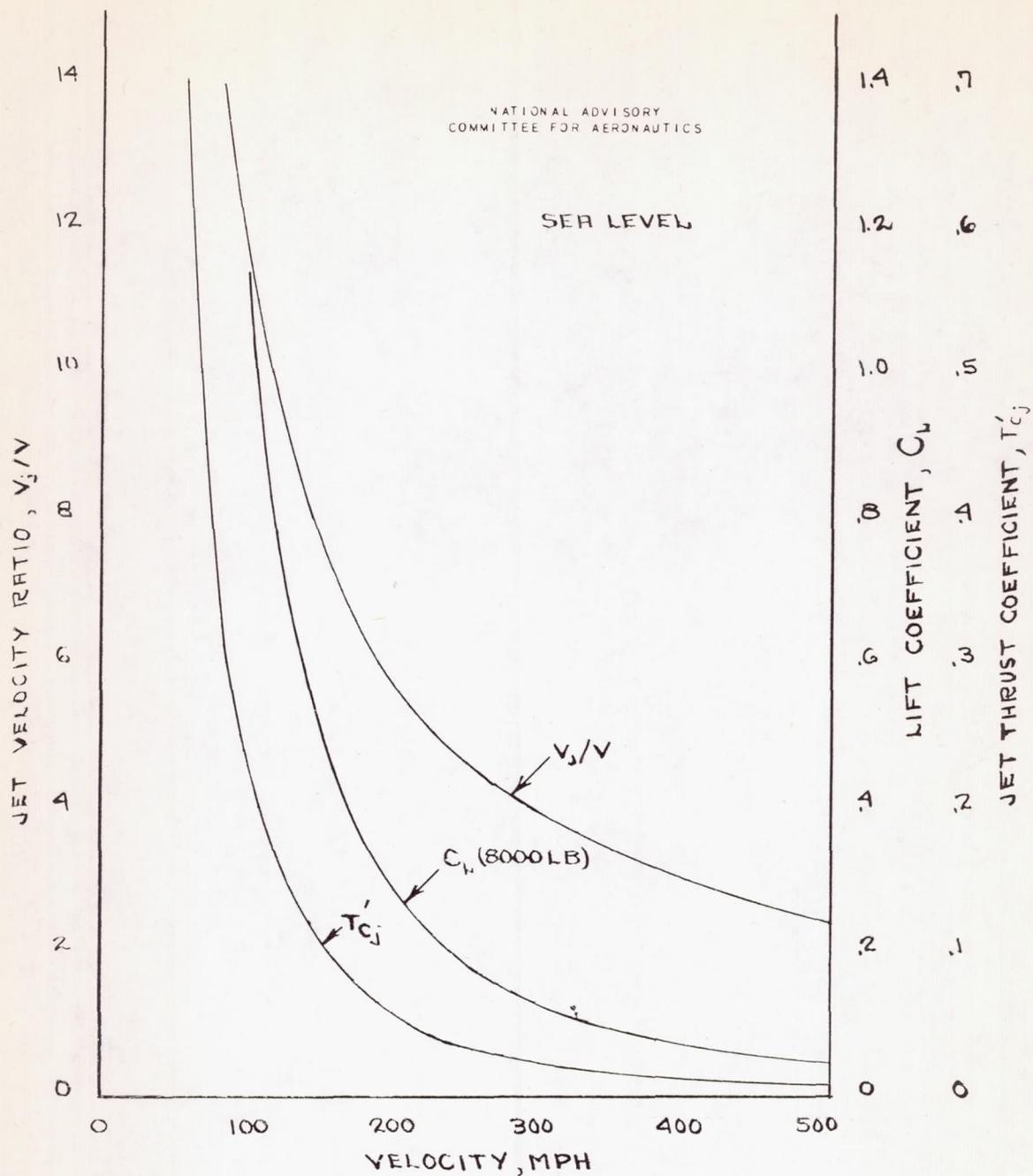
FIGURE 8 - MILITARY-RATED-POWER CHARACTERISTICS OF THE
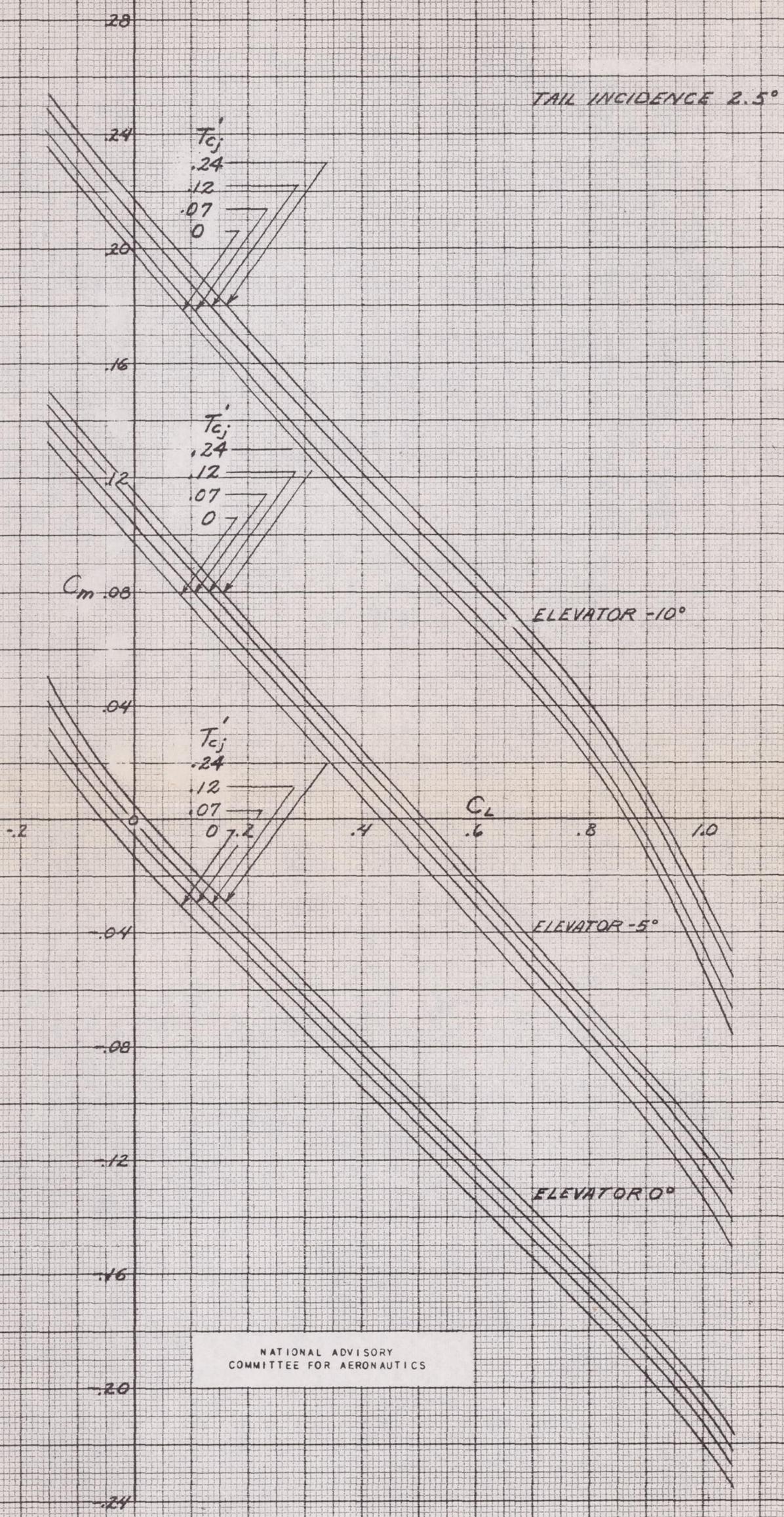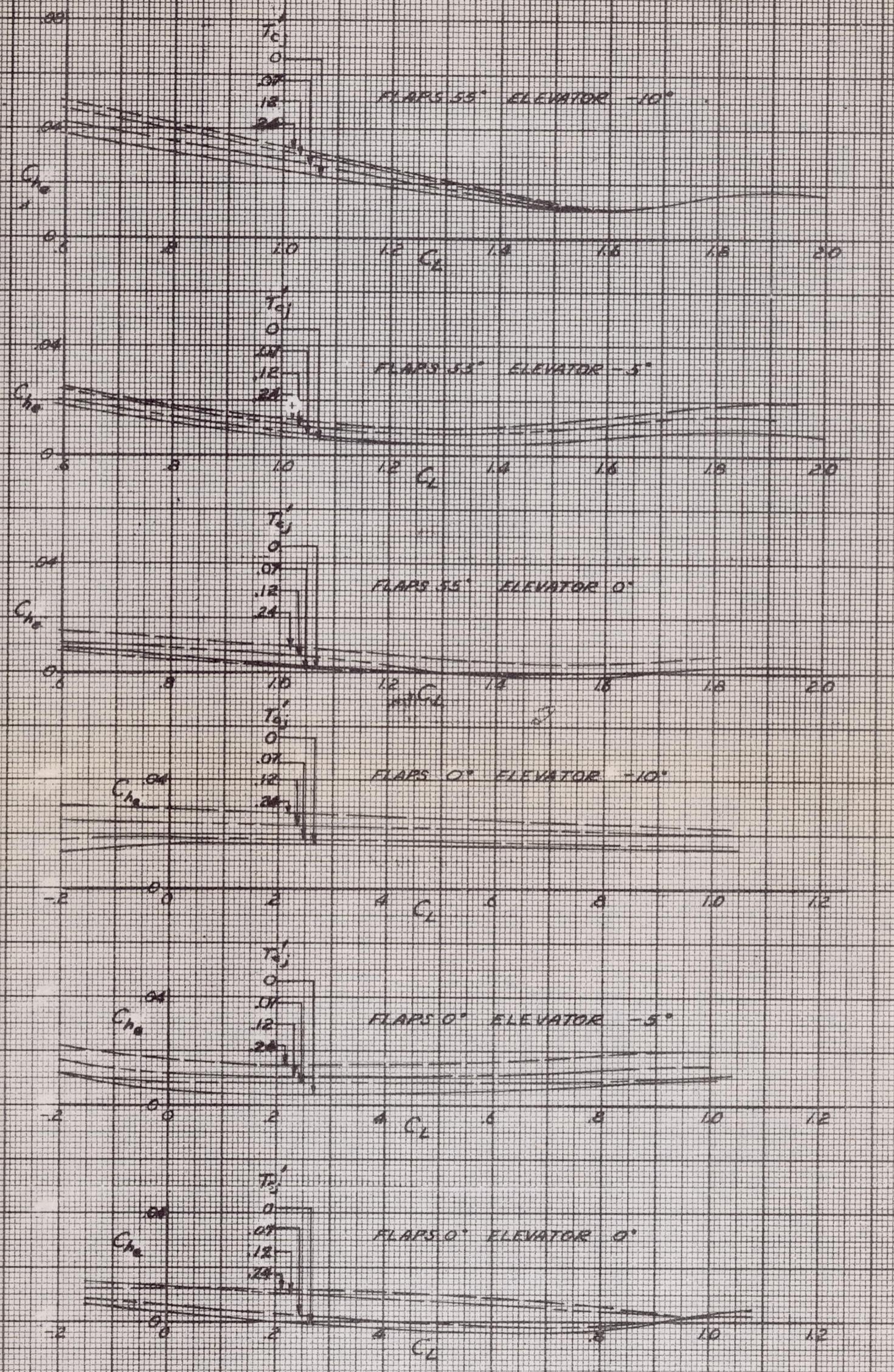JET-PROPULSION ENGINE OF THE SINGLE-ENGINE AIRPLANE

FIGURE 9. - VARIATION OF PITCHING-MOMENT COEFFICIENT WITH LIFT COEFFICIENT AT CONSTANT THRUST COEFFICIENT FOR THE SINGLE-ENGINE AIRPLANE MODEL. FLAPS RETRACTED

FIGURE 10.- VARIATION OF PITCHING-MOMENT COEFFICIENT WITH LIFT COEFFICIENT AT CONSTANT THRUST COEFFICIENT FOR THE SINGLE-ENGINE AIRPLANE MODEL. FLAPS DEFLECTED 25°
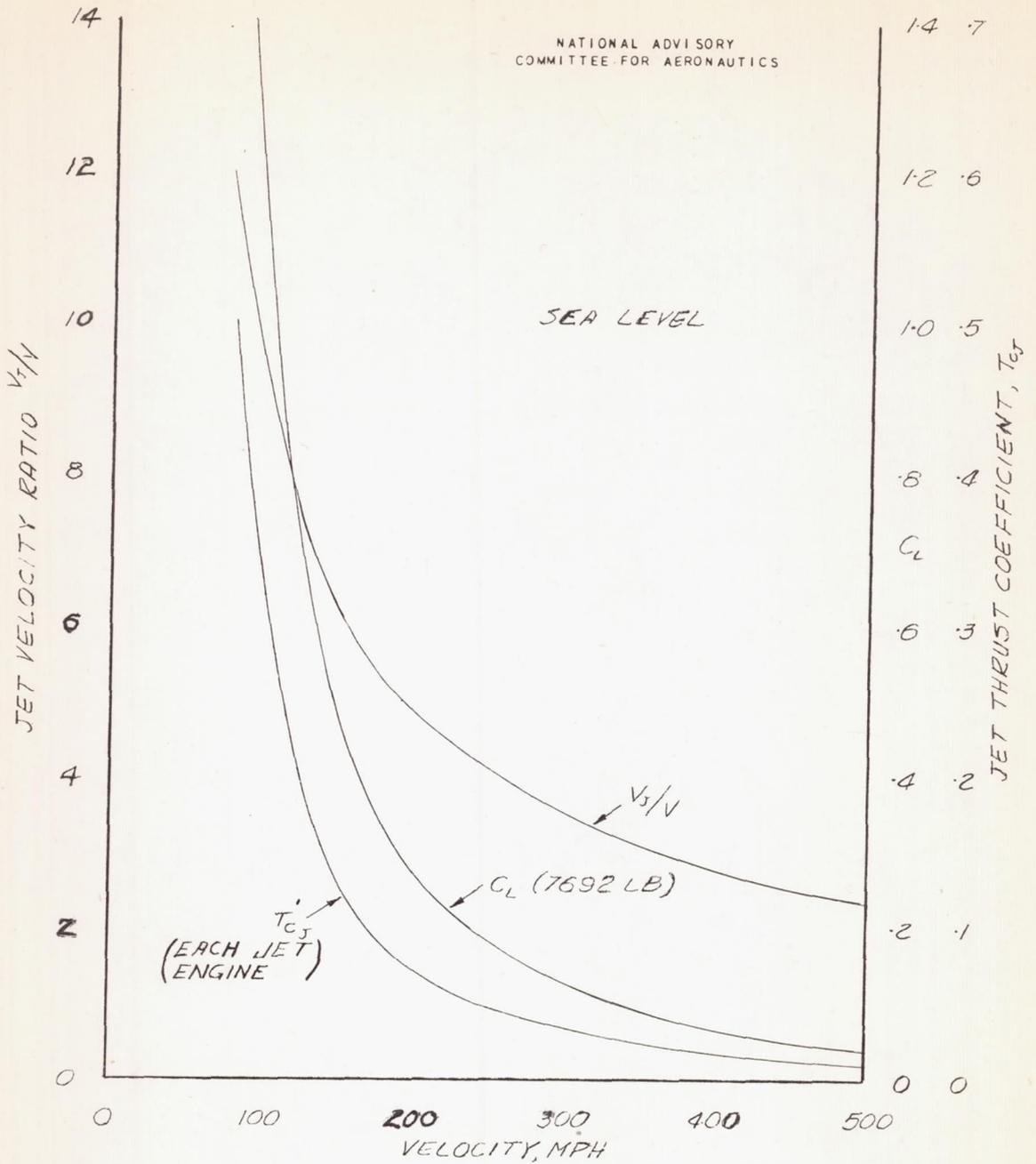
FIGURE 11.— VARIATION OF ELEVATOR HINGE-MOMENT COEFFICIENT WITH LIFT COEFFICIENT AT CONSTANT THRUST COEFFICIENT FOR THE SINGLE-ENGINE AIRPLANE MODEL.

FIGURE 12.— MILITARY-RATED-POWER CHARACTERISTICS
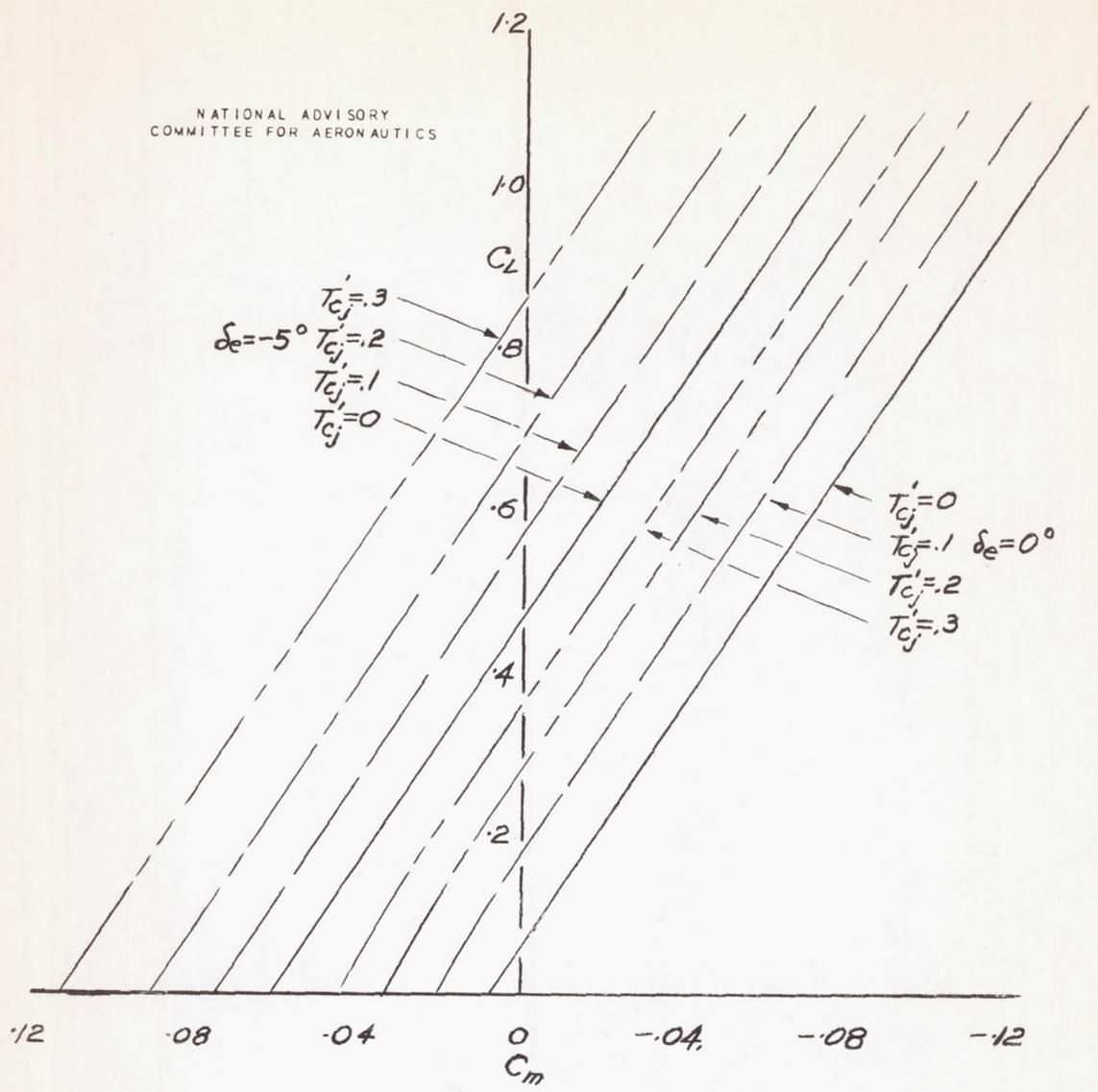OF THE JET-PROPULSION ENGINES OF THE
TWO-ENGINE AIRPLANE.

FIGURE 13.—VARIATION OF PITCHING-MOMENT COEFFICIENT WITH LIFT COEFFICIENT AT CONSTANT THRUST COEFFICIENT FOR TWO-ENGINE AIRPLANE MODEL. FLAPS RETRACTED.
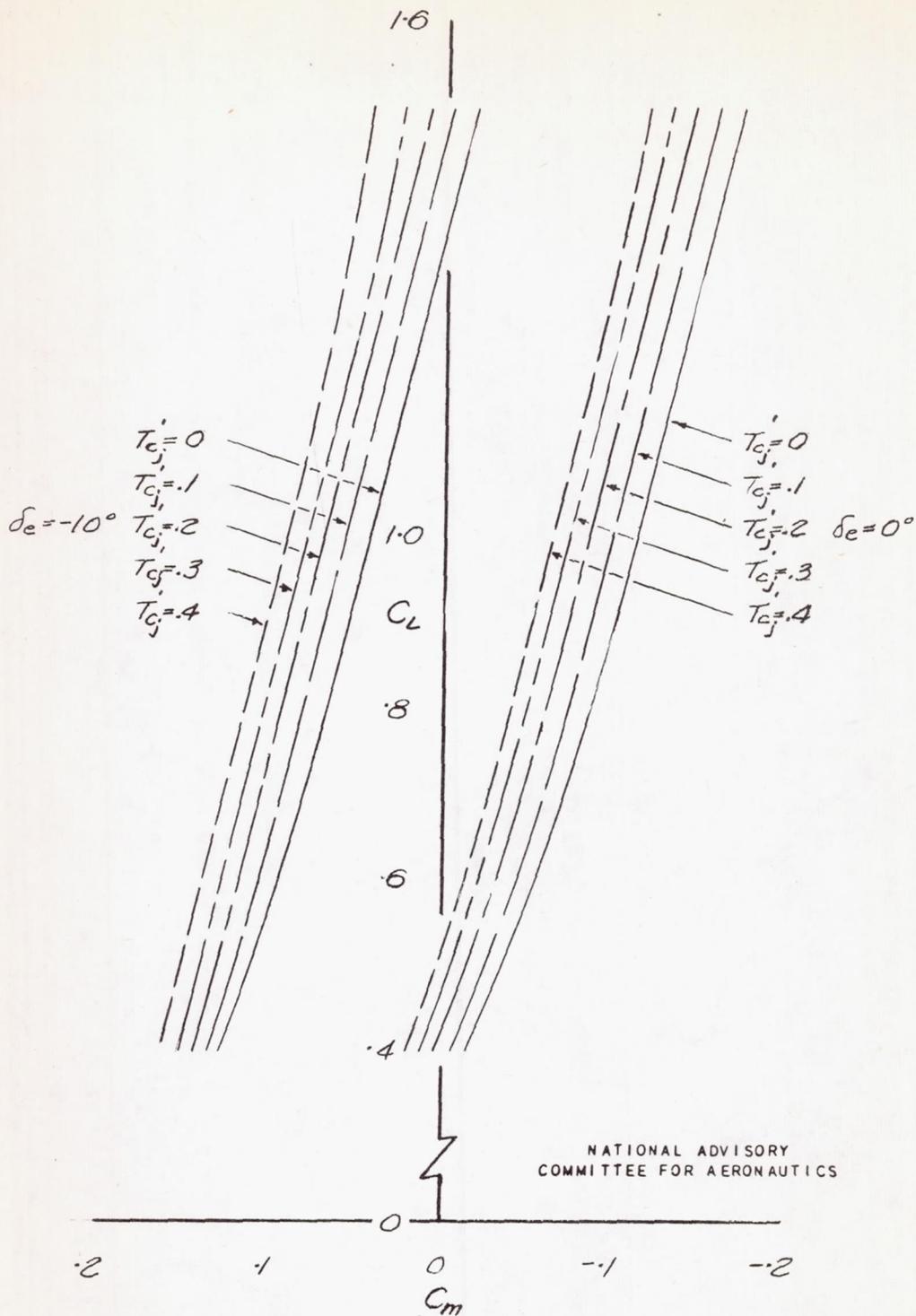
FIGURE 14.— VARIATION OF PITCHING-MOMENT COEFFICIENT
WITH LIFT COEFFICIENT AT CONSTANT THRUST
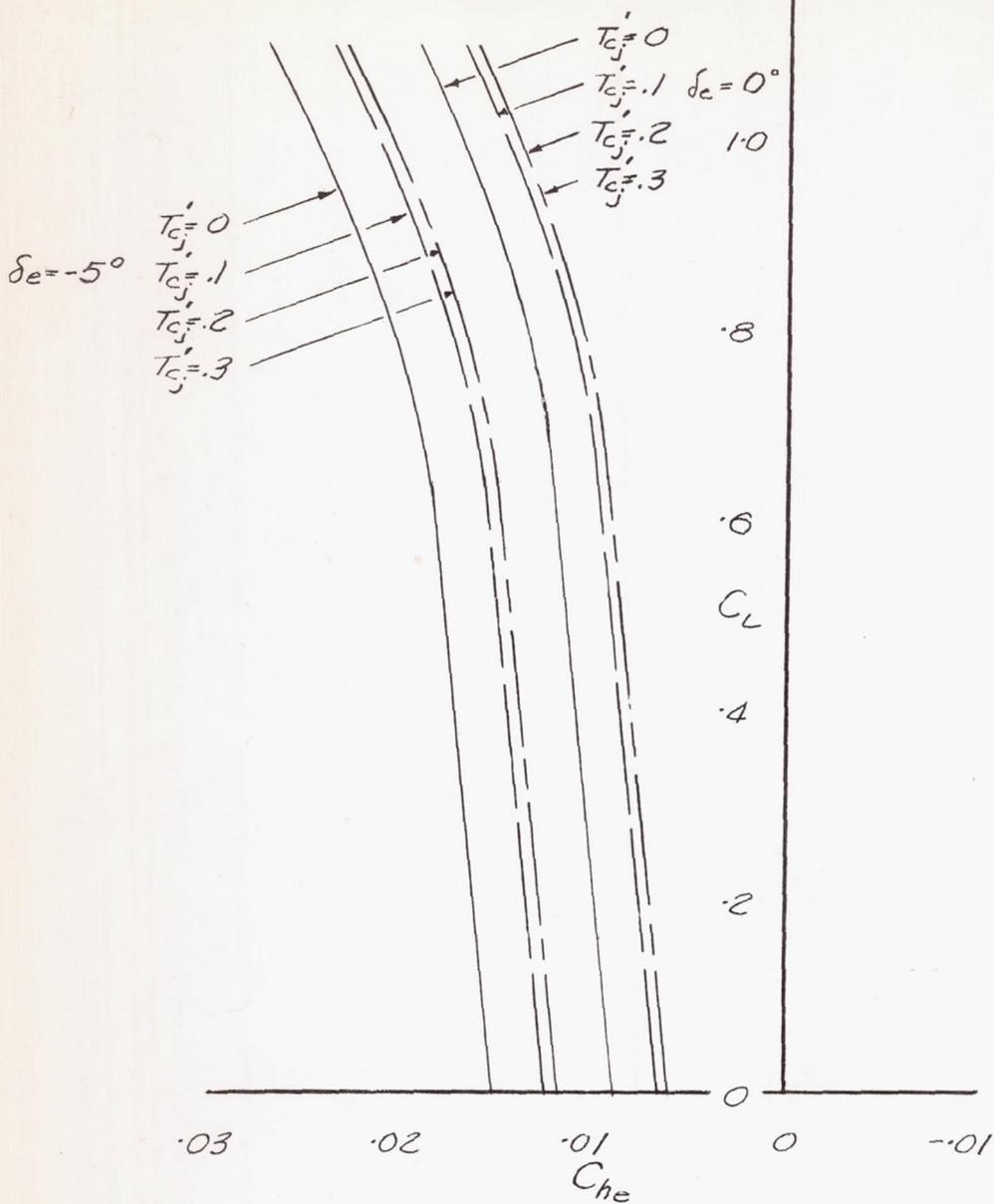COEFFICIENT FOR TWO-ENGINE AIRPLANE
MODEL. SPLIT FLAPS DEFLECTED 60°.

FIGURE 15.— VARIATION OF HINGE-MOMENT COEFFICIENT
WITH LIFT COEFFICIENT AT CONSTANT THRUST
COEFFICIENT FOR TWO-ENGINE AIRPLANE
MODEL. FLAPS RETRACTED.